Electronic Supplementary Material (ESI) for ChemComm.

Electronic Supporting Information (ESI)

Efficient Hydrogen Evolution from Hydrolysis of Ammonia Borane using Bilateral-like WO_{3-x} Nanorods Coupled with Ni_2P Nanoparticles

Yongbing Lou,*[a] Jinxin He,[a] Guoning Liu,[a] Shaopeng Qi,[a] Lin Cheng,[a] Jinxi Chen,*[a] Yixin Zhao*[b] and Jun-Jie Zhu*[c]

a. School of Chemistry and Chemical Engineering, Jiangsu Key Laboratory for Science and Application of Molecular Ferroelectrics, Jiangsu Engineering Laboratory of Smart Carbon-Rich Materials and Device, Southeast University, Nanjing, 211189, China, E-mail: lou@seu.edu.cn, chenjinxi@seu.edu.cn

b. School of Environmental Science and Engineering, Shanghai Jiao Tong University, Shanghai, 200240, China, E-mail: yixin.zhao@sjtu.edu.cn

c. State Key Lab of Analytical Chemistry for Life Science, School of Chemistry and Chemical Engineering, Nanjing University, Nanjing, 210093, China, E-mail: jjzhu@nju.edu.cn

Chemicals. Chemicals used include tungsten chloride (WCl_6, ≥99.9% trace metal basis, Aladdin), oleic acid (Technical Grade, 90%, Sigma Aldrich), trioctylamine (96%, Energy Chemical), Nickel acetylacetonate (95%, Aladdin), oleylamine (80-90%, Aladdin), 1-Octadecylene (90%, Sigma Aldrich), tri-n-octylphosphine (TOP, 90%, Aladdin). Ammonia borane (NH_3BH_3) was purchased from Macklin Co. All chemicals were purchased from commercial vendors and utilized without any further purification.

Synthesis of WO_{3-x} NRs. The synthesis of tungsten oxide NRs was carried out with standard Schlenk line techniques. In a 50 mL 3-neck flask, 0.92 mmol of WCl_6 was added to 10 mmol of oleic acid and 5.5 mmol of trioctylamine to form a mixture. Subsequently, using an electric mantle, the mixture was vigorously stirred and heated to 120 °C for 1 h under vacuum to eliminate other low-boiling impurities and water. After being transferred to the atmosphere of nitrogen, the flask was heated to 270 °C for 6 h. Until cooled to room temperature naturally, the dark blue product was collected by centrifugation at 4000 rpm, washed with 2:1 mixture of ethanol/n-hexane for several times to remove the residues of organic reagent and finally dried under vacuum at 65 °C for 12 h, waiting for further characterization and applications. The samples synthesized at 260 °C, and 270 °C were marked as WO_{3-x}-L and WO_{3-x}-H, respectively, based on their low and high LSPR peak intensities. WO_{3-x}-H was calcined under oxygen atmosphere at 450 °C for 2 h to form P-WO_3. C-WO_3 was the commercial WO_3 without any treatment.

Synthesis of Ni_2P NPs and WO_{3-x}/Ni_2P NHs. Ni_2P NPs were synthesized using a modified literature procedure.[1] Since the reaction is an air-sensitive reaction that was deemed as highly corrosive and dangerous, it was performed rigorously under inert atmosphere using glove-box and Schlenk techniques. In detail, 0.49 mmol of $Ni(acac)_2$ was added to a three-necked flask containing 1-octadecene (7.05 mmol) together with oleylamine (6.98 mmol) and in certain cases TOP with Ni to TOP ratio of 1:6. After sealing the flask, the reaction mixture was stirred moderately and evacuated for 15 min, then flushed with nitrogen for 5 min. Where after, the mixture was heated to 120 °C , using a heating mantle, evacuated for 15 min and introduced to nitrogen again. The above operation was repeated two times. Finally the reaction mixture was gradually heated to 300 °C and kept for 2 h in a flowing N_2. During the process of warming up, the reactants displayed a range of color changes from transparent clear celeste, army green to black, starting from 225 °C to the final temperature. Followed by cooling to room temperature, the obtained black products were centrifuged at 8000 rpm for 5 min and rinsed using a mixture of hexane/ethanol (1:2) for three times. The final NPs were dried overnight in vacuum at 60 °C. The diverse amounts of as-prepared WO_{3-x} NRs were added to multiple precursors of the Ni_2P catalyst to obtain a series of WO_{3-x}/Ni_2P nanohybrid catalysts, which were provided with different weight ratios of WO_{3-x} to Ni_2P. The samples were named as WO:NiP-n (n is the mass ratio of WO_{3-x} to Ni_2P). The mechanical mixtures of WO_{3-x} NRs and Ni_2P Nps were labeled as WO+NiP-n (n is the mass ratio of WO_{3-x} to Ni_2P). The performed operation steps of synthesized compound were the same as above.

Characterization. X-ray powder diffraction (XRD) measurement was performed on a Ultima IV diffractometer (Japan) equipped with Cu-Kα radiation (λ = 0.15406 nm). Transmission electron microscope (TEM) images and high-resolution transmission electron microscope (HRTEM) images were taken with a JEOL JEM-2100 at an acceleration voltage of 200 kV. Selected-area electron diffraction (SAED) and energy dispersive X-ray spectroscopy (EDX) were performed on a Tecnai G2 T20 with an energy dispersive spectrometry GENESIS XM2. UV-Vis-NIR absorption spectra was recorded on a UV-3600 spectrophotometer (Shimadzu). Photoluminescence (PL) measurements were conducted with a fluorescence spectrometer (Horiba, Fluoromax-4) at room temperature. X-ray photoelectron spectroscopy (XPS) spectra were recorded with a Thermo Scientific Escalab 250 Xi. Inductively coupled plasma atomic emission spectroscopy (ICP-AES) was measured using an iCAP 7400 Spectrometer (Thermo Fisher).

Catalytic activity measurement. The catalytic hydrogen evolution experiments were performed in a 127 mL quartz flask containing 80 mL of ammonia borane aqueous solution with magnetic stirring at 5 °C. Typically, 50 mg of the catalyst was firstly dispersed in 78 mL of distilled water. Subsequently, the filled flask was evacuated for 20 minutes and was injected with 20 mL of argon. Prior to irradiation, 2 mL of NH_3BH_3 (0.32 mmol) solution was injected into the suspension through a silica gel membrane. The experimental tests were carried out in visible light and dark conditions, respectively. And the visible light irradiation was provided by a 300 W Xe-lamp configured with 400 nm cut-off filter. The amount of H_2 was measured by gas chromatography (GB-9890, Argon gas as a carrier gas) using a thermal conductivity detector (TCD). Moreover, the prepared samples were calcined at 350 °C for 2 h under inert gas atmosphere prior to catalysis. Hydrogen evolution from high concentration of ammonia borane aqueous solution were monitored by using the classic drainage method. A certain amount of catalysts were ultrasonically dispersed in 2 mL of deionized water in a 10 mL two-necked round bottom flask. Next, a aqueous solution (3 mL) containing 1.62 mmol AB was injected into the flask through a rubber plug using a syringe. The reaction system was magnetically stirred and the reaction temperature was maintained using a water bath. The generated hydrogen was introduced through a conduit into a water-filled graduated cylinder for quantitative analysis. All hydrolytic dehydrogenation reactions were carried out under visible light ($\lambda \geq 400$ nm) unless otherwise specified.

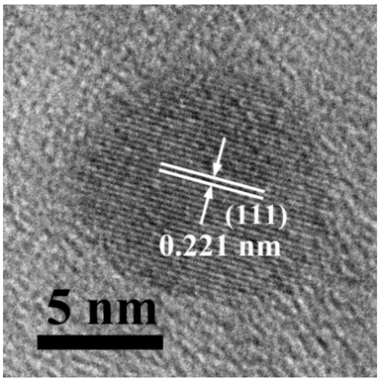

Fig. S1. High resolution TEM image of the prepared Ni_2P NP.

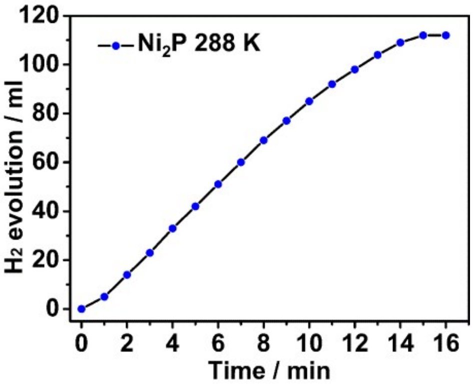

Fig. S2. Time courses of evolution of H_2 from aqueous solution (5 mL) containing 1.62 mmol AB for Ni_2P NPs (7 mg) treated by acetic acid at 288 K under visible-light irradiation (λ ≥400 nm). A short induction period was observed as the reaction was performed at a relatively high reaction concentration, where mass transportation may have played an important role for the reaction rate. The same phenomenon was also observed in some high-performance Ni_2P catalysts for the hydrolysis of AB according to the related documents.[2, 3]

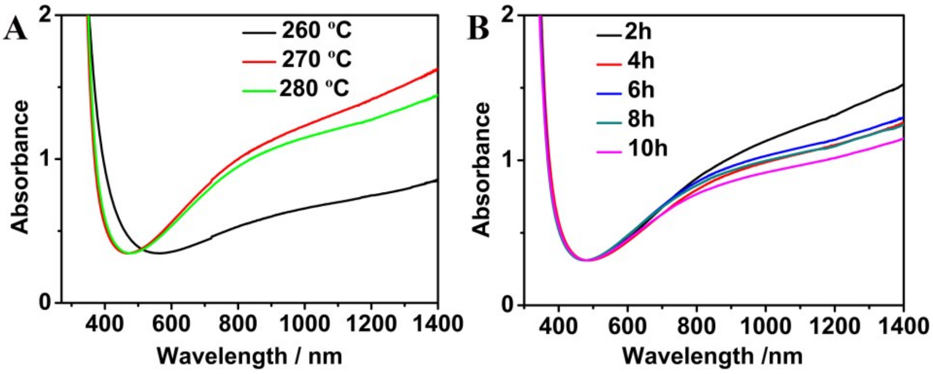

Fig. S3. (A) UV-Vis-NIR absorption spectrum of the WO_{3-x} obtained at 260 °C, 270 °C and 280 °C for 6 h. (B) UV-Vis-NIR absorption spectrum of the WO_{3-x} obtained at 270 °C for 2, 4, 6, 8, 10 h.

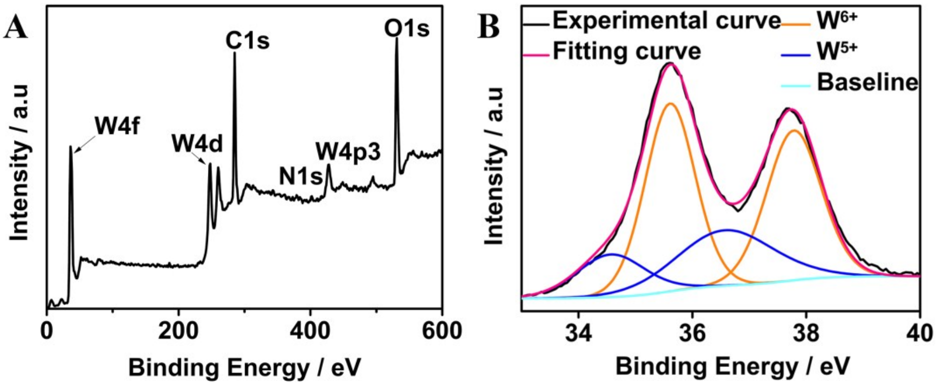

Fig. S4. XPS spectra: (A) Survey spectrum, (B) W4f spectra of WO_{3-x} obtained at 270°C for 6 h.

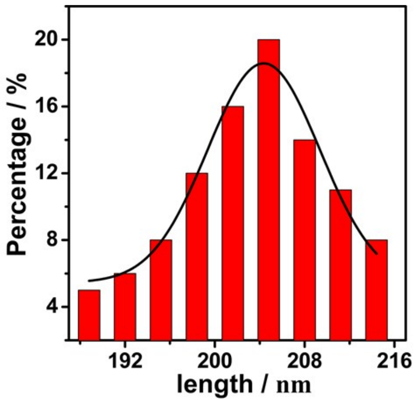

Fig. S5. The size distribution image of the WO_{3-x} NRs obtained at 270 °C for 6 h.

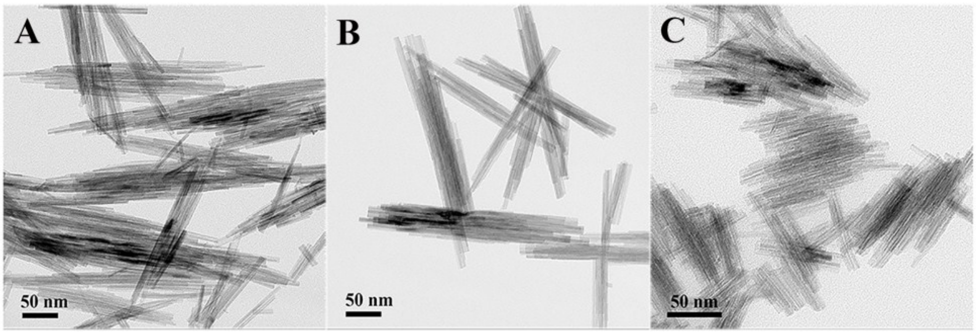

Fig. S6. TEM images of WO_{3-x} products obtained using a mixed ligand of oleic acid and trioctylamine in the volume ratio of (A) 5: 3, (B) 4: 4, and (C) 3: 5, respectively.

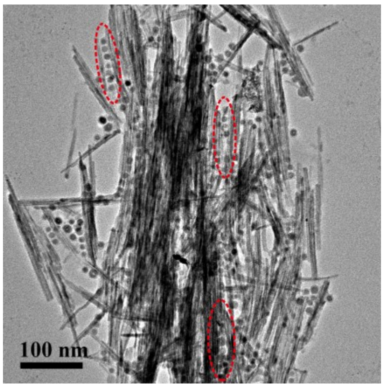

Fig. S7. TEM images of WO:NiP-4 NH.

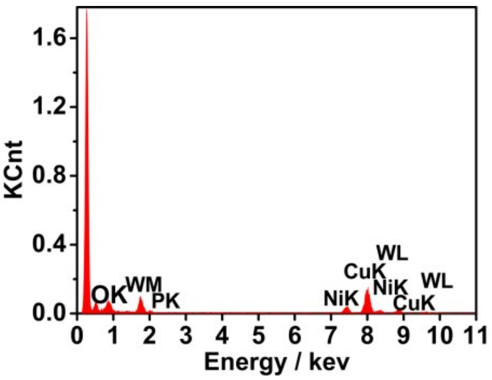

Fig. S8. EDX of WO:NiP-9 nanohybrid.

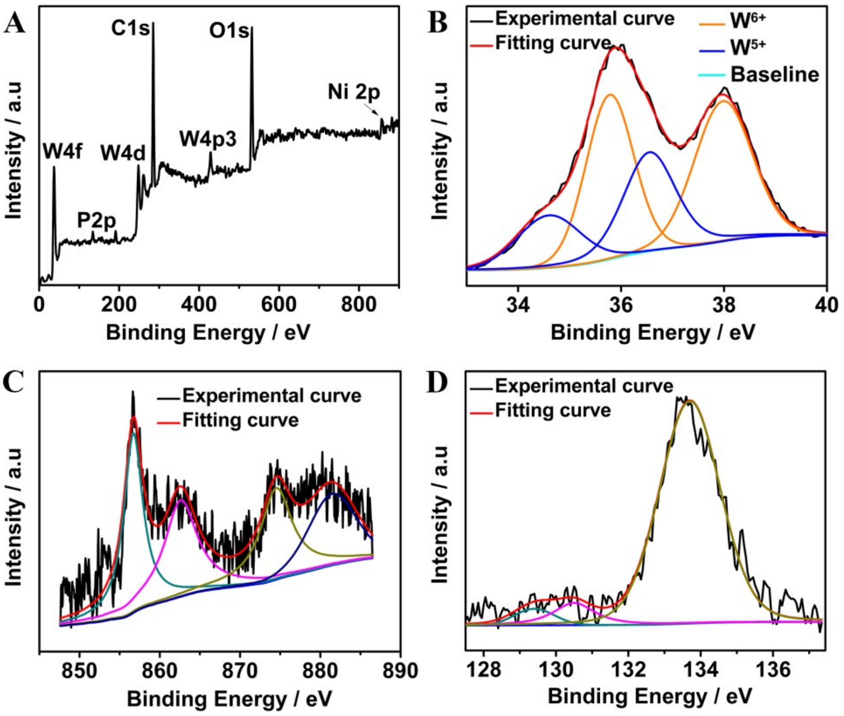

Fig. S9. XPS spectra: (A) Survey spectrum, (B) W4f spectrum, (C) Ni 2p spectrum and (D) P 2p spectrum of WO:NiP-9 nanohybrid. The two peaks with binding energies of 34.5 eV ($W4f_{7/2}$) and 36.6 eV ($W4f_{5/2}$) were assigned to W^{5+}. Two main satellite peaks founded at 856.7 eV (Ni $2p_{3/2}$) and 874.5 eV (Ni $2p_{1/2}$), which were consistent with those in Ni_2P. The spectrum of P 2p showed two peaks at 129.4 eV and 130.5 eV corresponding to P $2p_{3/2}$ and P $2p_{1/2}$ respectively, which are assigned to $P^{\delta-}$ in the Ni_2P. Another peak appeared at 133.7 eV is attributed to oxidized P species.

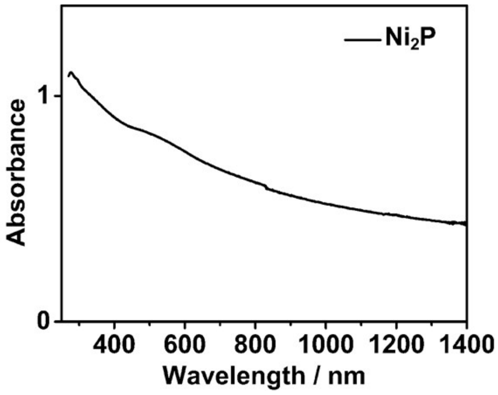

Fig. S10. UV-Vis-NIR absorption spectrum of the prepared Ni_2P NPs.

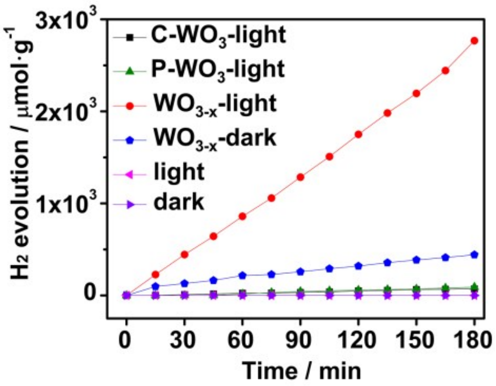

Fig. S11. Time courses of H_2 evolution from aqueous solution (80 mL) containing 0.32 mmol AB for different samples (50 mg) at 278 K under visible-light irradiation (λ ≥400 nm) and in the dark.

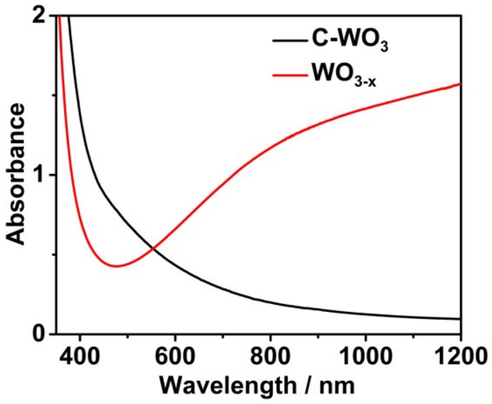

Fig. S12. The UV-Vis-NIR absorption spectra of WO_{3-x} NRs and commercial WO_3 powder (C-WO_3).

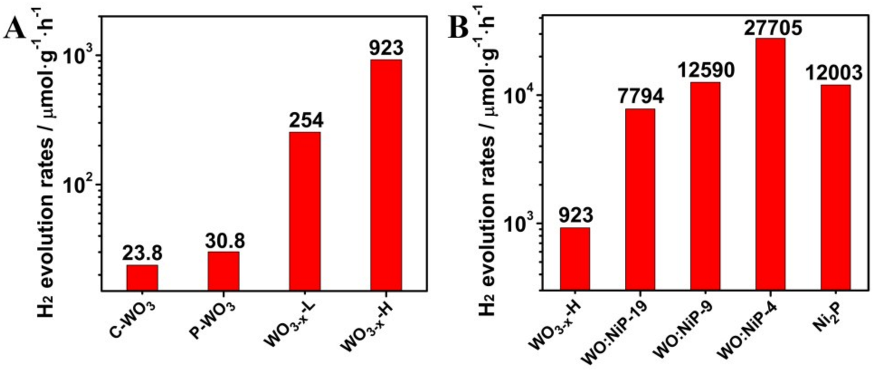

Fig. S13. (A) and (B) Catalytic activity of different samples (50 mg) annealed at 350 °C for hydrogen production from aqueous solution (80 mL) containing 0.32 mmol AB at 278K under visible-light irradiation (λ ≥400 nm). The catalytic performance of the WO_{3-x} NRs with intense LSPR was about 39 times higher than that of commercial WO_3 powder for H_2 generation, while the performance of plasmonic WO_{3-x} NR is still one order lower than those of the nanohybrids.

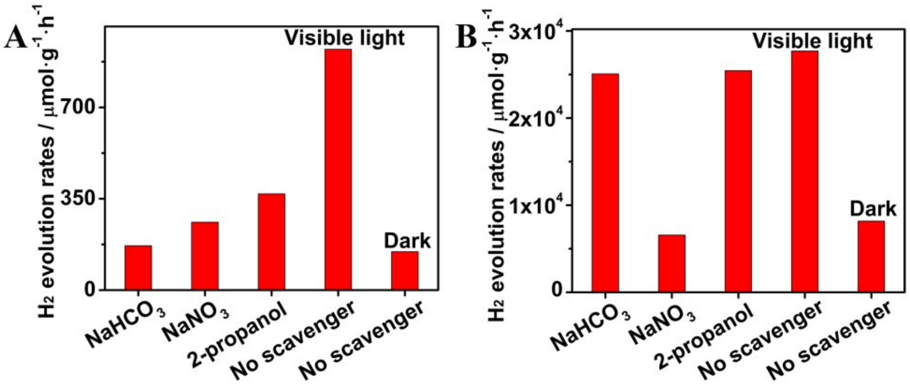

Fig. S14. The comparison of the catalytic hydrogen evolution rates in the presence and absence of scavengers from aqueous solution (80 mL) containing 0.32 mmol AB at 278 K under visible light over plasmonic (A) WO_{3-x} (50 mg) and (B) WO:NiP-4 hybrids (50 mg).

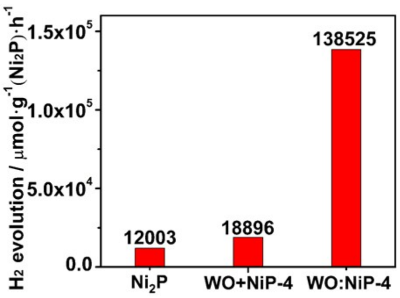

Fig. S15. Comparison of the catalytic H_2 evolution from 80 mL aqueous solution containing 0.32 mmol AB with 50 mg WO:NiP-4 NH, 50 mg mechanical mixture WO+NiP-4 (containing 40 mg WO_{3-x} NRs and 10 mg Ni_2P NPs), and 50 mg pure Ni_2P NPs at 278 K under visible light (λ ≥400 nm) .

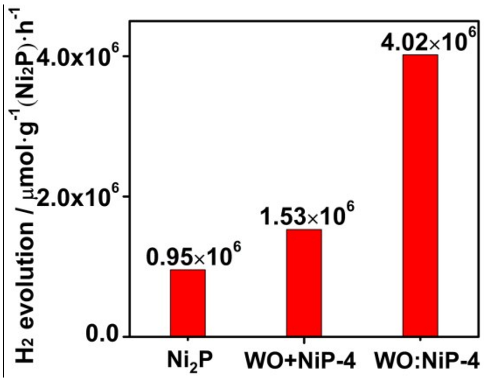

Fig. S16. Comparison of the catalytic H_2 evolution from 5 mL aqueous solution containing 1.62 mmol AB with 7 mg WO:NiP-4 NH, 7 mg mechanical mixture WO+NiP-4 (containing 5.6 mg WO_{3-x} NRs and 1.4 mg Ni_2P NPs), and 1.4 mg pure Ni_2P NPs at 289 K under visible light (λ ≥400 nm).

Table S1. Comparison of TOF values of different nickel-based catalysts for the catalytic hydrolysis dehydrogenation of ammonia borane.

No.	**catalyst**	**Experimental conditions**	**TOF $mol_{(H2)}\cdot mol_{(catalyst)}^{-1}\cdot min^{-1}$**	**Ref.**
1	Ni_2P NPs	288 K	8.16	this study
2	Ni_2P NPs	298 K (0.5 M NaOH)	About 16	2
3	Ni_2P NPs	298 K	40.4	3
4	Nanoporous Ni spheres	298 K	19.6	4
5	Ni NPs/ZIF-8	298 K (0 M NaOH)	35.3	5
6	Ni NPs/ZIF-8	298 K (0.3M NaOH)	85.7	5
7	Ni /ZIF-8	298 K	8.4	6
8	3.2 nm Ni/C	298 K	8.8	7

Reference:

1. E. J. Popczun, J. R. McKone, C. G. Read, A. J. Biacchi, A. M. Wiltrout, N. S. Lewis and R. E. Schaak, *J. Am. Chem. Soc.*, 2013, **135**, 9267.
2. C.-C. Hou, Q. Li, C.-J. Wang, C.-Y. Peng, Q.-Q. Chen, H.-F. Ye, W.-F. Fu, C.-M. Che, N. López and Y. Chen, *Energy Environ. Sci.*, 2017, **10**, 1770.
3. C. Y. Peng, L. Kang, S. Cao, Y. Chen, Z. S. Lin and W. F. Fu, *Angew. Chem. Int. Ed.*, 2015, **54**, 15725.
4. C. Y. Cao, C. Q. Chen, W. Li, W. G. Song and W. Cai, *ChemSusChem*, 2010, **3**, 1241.

5. C. Wang, J. Tuninetti, Z. Wang, C. Zhang, R. Ciganda, L. Salmon, S. Moya, J. Ruiz and D. Astruc, *J. Am. Chem. Soc.*, 2017, **139**, 11610.
6. P. Z. Li, K. Aranishi and Q. Xu, *Chem. Commun.*, 2012, **48**, 3173.
7. Ö. Metin, V. Mazumder, S. Özkar and S. Sun, *J. Am. Chem. Soc.*, 2010, **132**, 1468.